Electronic Supplementary Material (ESI) for Journal of Materials Chemistry C.

Supporting information

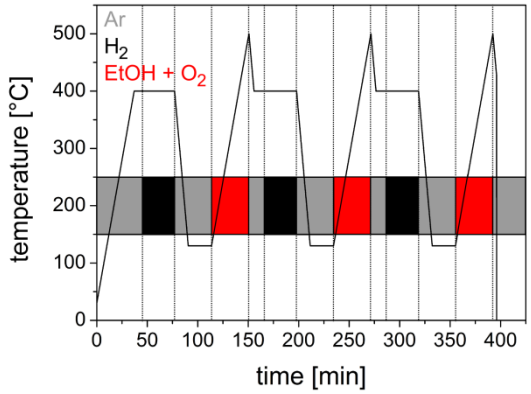

Fig. S1 Complete temperature *vs.* time intervals together with the corresponding gas atmospheres during each interval for the temperature programmed (TP) catalysis experiments.

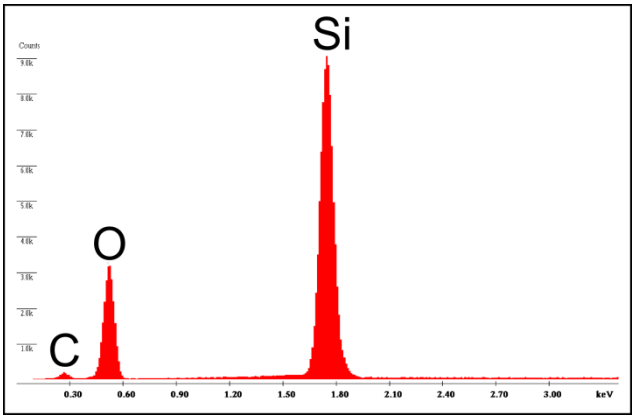

Fig. S2 EDX spectrum of silica hollow spheres.

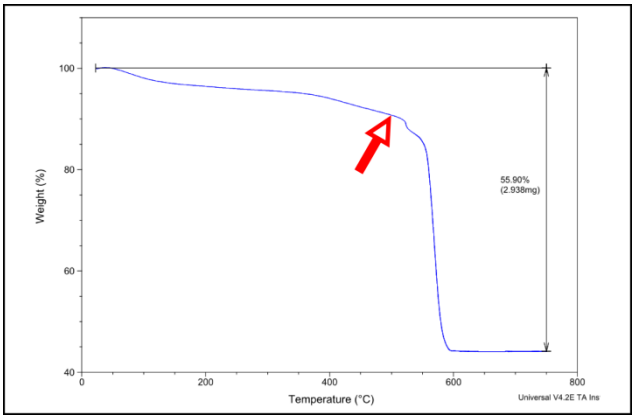

Fig. S3 TGA of PS/silica CS spheres under synthetic air (O_2/N_2 = 20/80 w/w) in the temperature range of 25-750 °C, heated to 500 °C at maximum heating power (red arrow), and then heated to the final temperature with a heating rate of 3 K/min. The weight loss is completed at 590 °C. Up to the final temperature of 750 °C, the mass remains constant corresponding to the expected value of pure silica of 44 wt%. For the TGA measurements the thermogravimetric analyser TGA Q-500 (TA Instruments, Eschborn) was used.

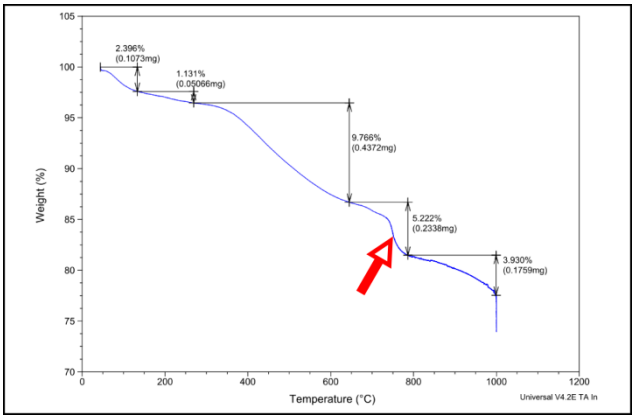

Fig. S4 TGA of PS/silica CS spheres under synthetic air (O_2/N_2 = 20/80 w/w) in the temperature range of 25-1000 °C, heated to 750 °C at maximum heating power (red arrow), and then heated to the final temperature with a heating rate of 3 K/min. The weight loss is not fully completed until the final temperature of 1000 °C is reached, but there remains a large residue of 77.6 wt% of the initial mass. Apparently the product still contains any residues of the PS. For the TGA measurements the thermogravimetric analyser TGA Q-500 (TA Instruments, Eschborn) was used.

Tab. S5 Results of the C/O elemental analysis of PS/silica CS spheres after calcination at different temperatures.[a]

temperature (°C)	C content (mol%)	O content (mol%)	Si content (mol%)
550	< 0.8	65.5	> 33.7
750	45.8	33.2	21.0

[a] Chemical composition was characterized by usual combustion elemental analysis for C using the C analyser LECO C-200 (LECO Instrumente GmbH, Mönchengladbach) and by hot gas extraction for O using the N/O analyser LECO TC-436 (LECO Instrumente GmbH, Mönchengladbach); Si content was back-calculated by taking into account the C and O content.

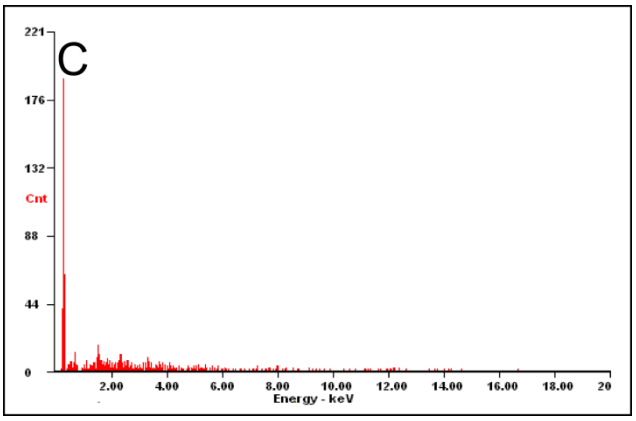

Fig. S6 EDX spectrum of carbon hollow spheres.

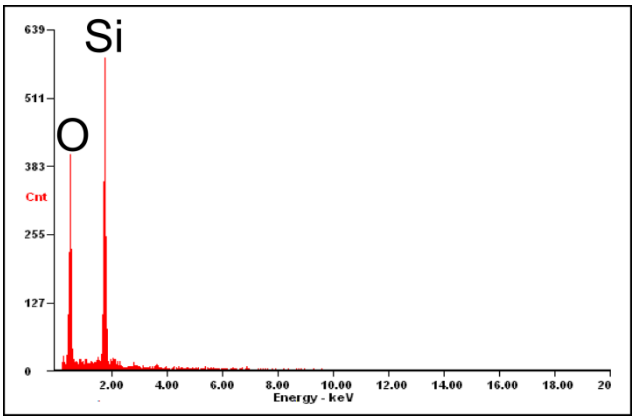

Fig. S7 EDX spectrum of silica hollow fibres.

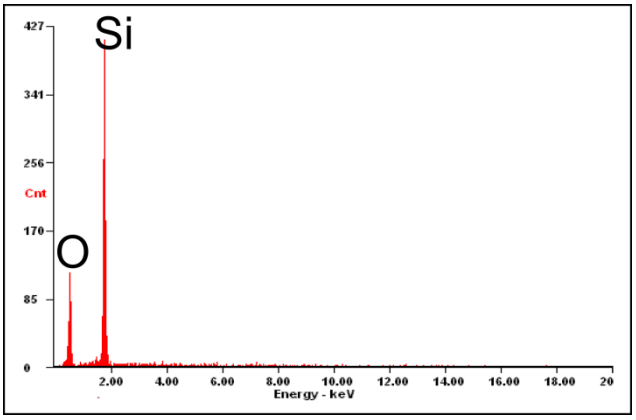

Fig. S8 EDX spectrum of porous silica layer with channel pores.

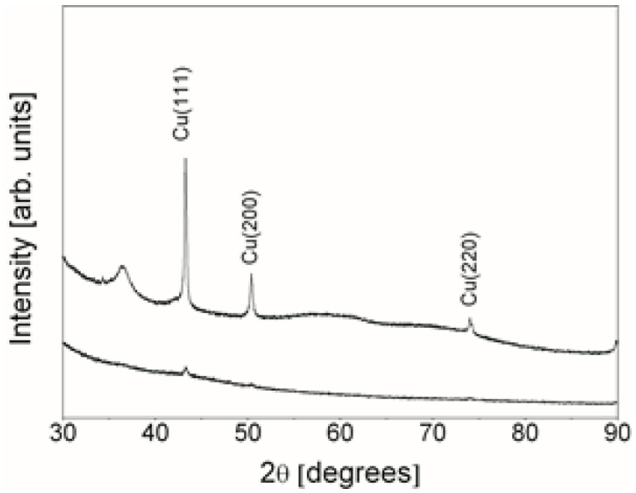

Fig. S9 Powder XRD of the metallic copper particles deposited on the amorphous silica membrane with channel pores ($Cu@SiO_2$) by impregnation/calcination/reduction procedure. Additional broad and featureless signals at 2 Φ 36° and between 55° and 60° are due to substrate signals. XRD measurement was performed using StadiP instrument (StadiP, Stoe & Cie GmbH, Darmstadt) in Debye-Scherrer mode (flat specimen, transmission mode) with Co-$K\alpha_1$-radiation and a Ge(111) monochromator.

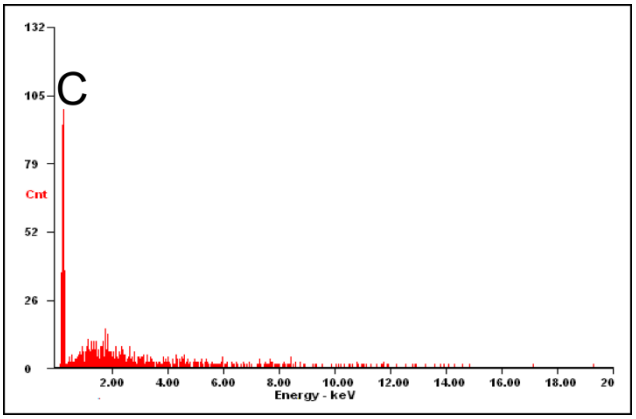

Fig. S10 EDX spectrum of porous carbon layer with tubular structured pores.

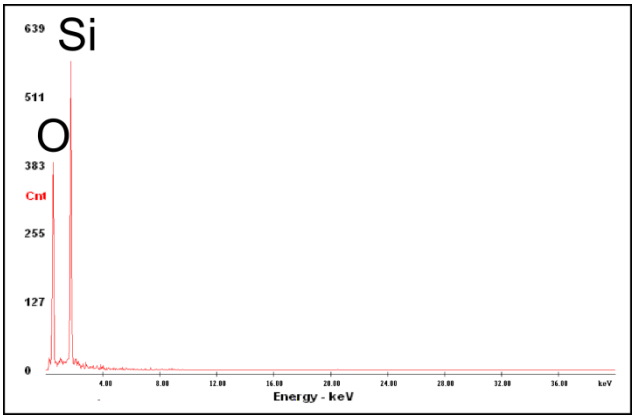

Fig. S11 EDX spectrum of silica 3DOM structure.

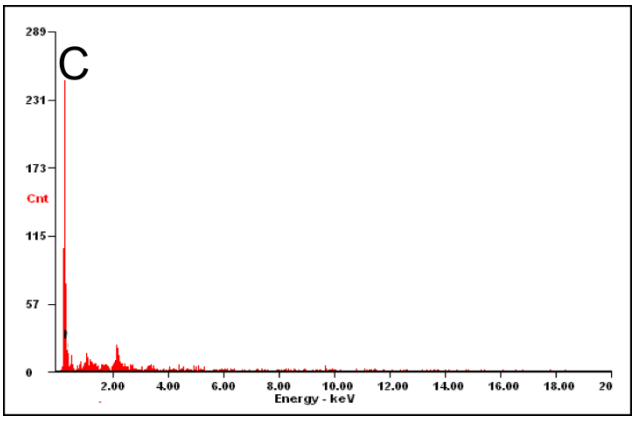

Fig. S12 EDX spectrum of carbon 3DOM structure.

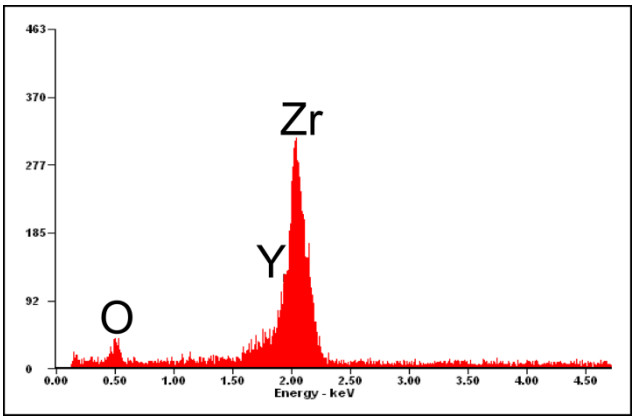

Fig. S13 EDX spectrum of porous YSZ layer with channel pores.

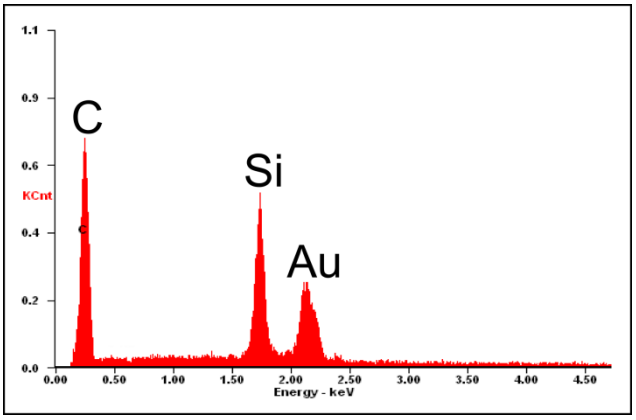

Fig. S14 EDX spectrum of porous SiC layer with tubular structured pores (Note: the Au signal in the EDX spectrum comes from specimen coating with Au for SEM measurements and is not a component of the micro-/nanostructure).